Sustainable leather finishing: optimizing thermal properties with graphene nanoplatelet-polyurethane nanocomposites

R. Mascolo[1], C. Siviello[2], F. Bertocchi[2], C. Azzaretto[3], F. Cilento[4], B. Palmieri[4], A. Martone[4]

[1] Stazione Sperimentale per l'Industria delle Pelli e delle Materie Concianti srl, via Campi Flegrei 34, 80078 Pozzuoli, Napoli, Italy, r.mascolo@ssip.it
[2] Jaber Innovations srl, Area Sviluppo Industriale 81030 Teverola (CE), Italy, ciro.siviello@jaber.it
[3] Pasubio SpA, Via Seconda Strada 38, 36071 Arzignano (VI), Italy, claudio.azzaretto@pasubio.com
[4] Institute for Polymers Composites and Biomaterials, National Research Council of Italy, P.le E Fermi,1 80055 Portici (NA) Italy, alfonso.martone@cnr.it

ABSTRACT

The leather industry is facing increasing demands for sustainable, high-performance materials that enhance comfort while minimising environmental impact. Traditional leather coatings often compromise breathability and thermal regulation, affecting wearer comfort, while the use of synthetic polymers raises ecological concerns. This study investigates a novel approach by incorporating graphene nanoplatelets (GNPs) into polyurethane (PU) coatings for leather finishing, aiming to improve thermal management, durability, and sustainability.

Two GNP variants with different aspect ratios (low and high) were dispersed in a PU matrix at various concentrations to evaluate their impact on coating performance. Thermal diffusivity was measured using an IR camera with a 1W LED heat source, while mechanical properties were tested through tensile analysis. Results showed that low-aspect-ratio GNPs, when used above the percolation threshold, significantly enhanced heat dissipation without compromising flexibility. This formulation also showed better dispersion and interfacial adhesion than high-aspect-ratio GNPs, which tended to aggregate at higher concentrations.

The optimized GNP-PU coating improves thermal comfort—critical for automotive and apparel applications—while reducing the need for excessive synthetic additives by achieving performance gains at lower filler loadings. These findings demonstrate the potential of nanomaterial-enhanced coatings to address both functional and environmental challenges, offering a more sustainable path for leather product development. Further research should assess the long-term durability and broader application potential of these nanocomposite coatings.

Keywords: Sustainable leather, graphene nanoplatelets, thermal comfort, polyurethane finishings, nanocomposites, eco-friendly materials.

1 Introduction

In the leather industry, the application of finishing represents a critical stage of production. This process employs binders, pigments, auxiliaries, and other components to enhance both the aesthetic appeal and the mechanical performance of leather. However, changing consumer expectations increasingly challenges conventional leather products, creating demand for functional finishing systems. Among these, antimicrobial properties are of particular interest, as microbial growth (e.g., bacteria and fungi) during prolonged use, especially in garments, can compromise durability, hygiene, and perceived value. Antibacterial coatings thus offer an effective approach to extending leather's service life and improving user safety (Mohamed *et al*., 2009).

Nanotechnology has gained significant attention in leather processing, particularly in tanning and finishing operations, due to the unique features of nanomaterials. Their nanoscale dimensions and high specific surface area enable deeper penetration into collagen fibers, improving structural integrity and functional properties (Fan, Ma, & Xu, 2019; Kothandam *et al*., 2016). Nanomaterials such as gold, zinc, copper, and titanium can be engineered in various morphologies, allowing targeted modifications to improve durability, flexibility, and resistance to degradation (Zheng, Nicovich, & Dickson, 2007). The performance of nanomaterials in leather finishing is strongly dependent on their structural and compositional characteristics, including particle size, size distribution, and elemental composition.

Among carbon-based nanomaterials, graphene derivatives offer outstanding potential due to their high aspect ratio, superior thermal and electrical conductivity, and excellent mechanical reinforcement capabilities (Kiranakumar *et al*., 2024; Sharma *et al*., 2024). While reduced graphene oxide (rGO) has been widely studied, graphene nanoplatelets (GNPs) are more suitable for industrial applications. Compared to rGO, GNPs exhibit higher intrinsic conductivity, fewer structural defects, and better processability. Furthermore, their hydrophobic nature facilitates dispersion in polymeric matrices, and their production through top-down exfoliation routes ensures cost-effective scalability. These advantages make GNPs preferable for applications in coatings, conductive composites, and energy systems, where consistent quality and high performance are required (Jakhmola, Das, & Dutta, 2024; Kaur, Verma, & Mehta, 2025; Soon *et al*., 2025).

In this work, two types of GNPs with different aspect ratios (1,500 and 500) were used as fillers of finishing layers for leather to develop a multilayer functional coating. The objective was to enhance the mechanical performance of the finishing layer while simultaneously improving its thermal conductivity. Experimental characterization confirmed that the incorporation of GNPs increased both mechanical strength and thermal diffusivity, demonstrating the potential of GNP-based functional coatings for high-performance leather applications.

2 Materials and Methods

2.1 Preparation of Nanocomposites as Leather Finishing

Two graphene nanoplatelet (GNP) grades with different aspect ratios were selected for this study. Both materials were kindly supplied by Nanesa Srl (Arezzo, Italy). The first grade, G2Nan, exhibits a high aspect ratio of approximately 1500, with an average lateral size of 30 µm and a thickness of 14 nm. The second grade, G7Nan, has an aspect ratio of about 500, with an average lateral size of 16 µm and a thickness of 21 nm. Table 1 summarises the main physical properties of the two nanoparticle types.

Table 1 – GNP Nanoparticle properties

DESCRIPTION	G2NAN	G7NAN
Average lateral size	D59 = 25 µm	D90 = 16 µm; D50 = 7 µm
Average flake thickness	14 nm (42 layers)	21 nm (63 layers)
Bulk density (g/cm^3)	0.020 – 0.042	0.2
Carbon content (%)	> 97	> 65
State	Water paste	Powder

The finishing polymers were formulated according to a research recipe provided by Pasubio S.p.A. (Arzignano, Italy), using a polyurethane-based base coat without pigments.
A laboratory-scale coating process was performed using spray deposition to develop the multilayer finishing system. The finishing structure consists of five layers applied sequentially: Top Coat #2, Top Coat #1, Base Coat #2, Base Coat #1, and Primer (Figure 1). Among these, only the base coat layers were functionalized with graphene nanoplatelets (GNPs). The base coats are polyurethane-based, in line with typical automotive finishing formulations, while the top coats act as fixing layers based on isocyanate chemistry.
For the preparation of the modified base coats, GNPs were first blended with the polyurethane resin and subsequently dispersed using pulsed ultrasonication. This process serves two purposes: to promote deagglomeration of GNP clusters, ensuring uniform dispersion within the polymer matrix, and to partially fragment larger nanoplatelet stacks into smaller units. Reducing the size of GNP aggregates is essential because excessively large particles can induce surface defects, such as roughness or imprint marks, compromising both the aesthetic and functional properties of the final coating.

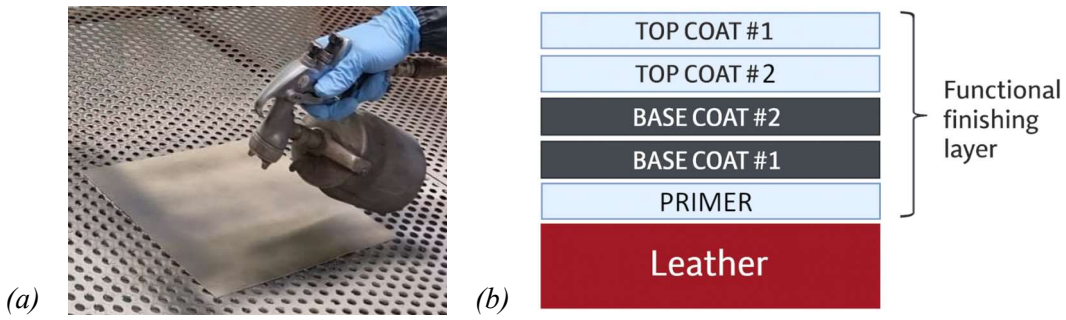

Figure 1 – Multilayer coating spray application (a) and layers stacking (b)

The composition of the multilayer coating system is detailed in Table 2. To enable the characterization of the multilayered coating, square specimens measuring 300 mm × 300 mm were prepared by spray deposition onto silicon substrates in order to ensure the proper detachment of the film from the substrate for subsequent mechanical, thermal, and thermomechanical characterization. Before application, the viscosity of each coating formulation was adjusted using a Ford Cup #5 to achieve a flow time of 20–25 seconds (corresponding to a viscosity between 100 cP and 120 cP), ensuring proper application and uniform layer formation. After the deposition, each layer underwent an intermediate drying stage in a convection oven at 70 °C for 60 seconds to promote solvent evaporation and avoid interlayer defects before the subsequent coating was applied.
The actual experimental configurations of the functional layers, reported in Table 2, describe the GNPs concentrations for the two nanoplatelet grades (G7Nan and G2Nan) as weight percentages relative to the base coat. These concentrations were selected according to the electrical percolation threshold of each GNPs type, providing sufficient nanoparticle networking within the coating matrix to potentially enhance functional properties while preserving the structural integrity and surface quality of the finishing system.

Table 1 – Modified multilayer finishing composition

LAYER	COATING WEIGHT (g/m²)	G7Nan wt%	G2Nan wt%
TOPCOAT #2	27.5	–	–
TOPCOAT #1	27.5	–	–
BASE COAT #2	55.0	18.0	4.5
BASE COAT #1	55.0	18.0	4.5
PRIMER	33.0	–	–

2.2 *Experimental characterization methods*

Thermogravimetric analysis (TGA) was carried out using a TA Instruments Q5000 (New Castle, DE, USA) in accordance with ASTM E 1131 to determine the thermal stability of the multilayer coating. Trials were performed under a nitrogen atmosphere with a heating rate of 10 °C/min from room temperature to 900 °C, using samples of approximately 15 mg. The residual weight and weight loss were recorded, regarding the mass loss at 750 °C.
Each multilayer coating (neat and modified with GNPs) was analysed using Differential Scanning Calorimetry (DSC) analysis was performed using a TA Instruments DSC Q2000 under a nitrogen atmosphere. Approximately 10 mg of each sample were sealed in aluminium pans. Specimens were subjected to two heating/cooling cycles from − 50 °C to 280 °C at 10 °C/min. The glass transition temperature (T_g) and enthalpy variations were determined from the DSC curves in accordance with ASTM D 3418.
Tensile tests have been performed using Dynamic Mechanical Analysis (DMA) techniques using a TA Instruments Q850 in tension film mode. Rectangular test pieces measuring (20.0 ± 0.10 mm × 6.0 ± 0.10 mm) were tested in *quasi-static* conditions at a displacement rate of 1 mm/min at two reference temperatures at 23 °C and 60 °C. Young Modulus was assessed in the 0.05 % and 0.25 % of strain.

2.3 *Nanoindentation tests on finished leathers*

Nanoindentation tests were carried out using a NanoTest platform (Micro Materials Ltd., Wrexham, UK), which records the dynamic load and displacement of a three-sided pyramidal diamond indenter (Berkovich tip, radius ≈100 nm). The tests were performed in force-controlled mode by applying a load in the range of 0.03–1.00 mN at a rate of 1 $mN \cdot s^{-1}$. Both loading and unloading curves were recorded. To minimize substrate effects, the maximum indentation depth was limited to less than 10% of the sample thickness. After load removal, the indenter was fully retracted to its initial position. The reduced modulus (E_r) was calculated from the slope of the unloading curve, while the sample stiffness was related to the Poisson's ratio and the tip geometry (Pharr *et al*. 1992).

2.4 *Thermal diffusivity tests on functionalized finished leather*

After the characterization of the multilayer coatings, they have been applied on a crust leather substrate to measure the improvement in thermal properties of finished leather.

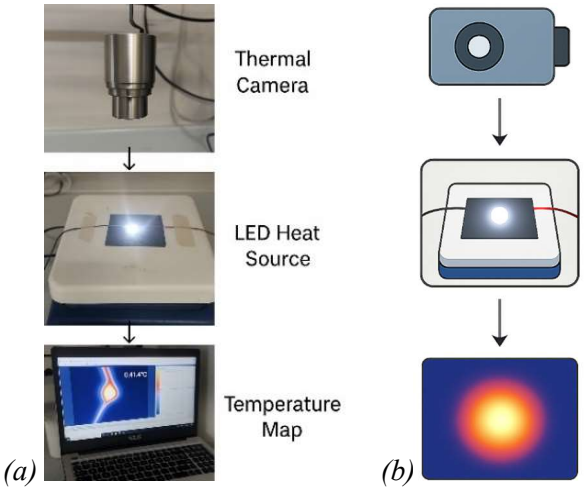

Figure 2 - Thermal diffusivity test (a) set-up and schematic (b)

To assess the thermal properties, a custom procedure was developed using an LED source as a controlled heat input. The LED (7 mm diameter, 1 W of power) was powered by a source meter at 3.7 V to ensure constant and repeatable input power. Samples were fixed on a flat ceramic-insulated surface to minimize external thermal interferences. The LED was placed in direct contact with the sample, applying heat for a standardized duration of 4 min to achieve a stable thermal gradient.
Thermal imaging was conducted using an infrared camera, Optris Xi 400, with the analysis software PIX Connect v. 3, to measure surface temperature distribution at regular intervals and enable the creation of thermal maps for heat diffusion analysis.
Two configurations were tested to evaluate thermal diffusivity, both in-plane (surface diffusivity) and through-plane (bulk diffusivity):

- *In-plane measurement*: the heat source was placed on the finished surface, and temperatures were recorded on the same side.
- *Cross-plane measurement*: the heat source was applied to the finished surface, while temperature was measured on the opposite side.

These tests provided data on heat distribution uniformity and rate, allowing indirect estimation of thermal capacity and conductivity.

3 Results and Discussion

3.1 Characterisation of nanocomposite multilayer coatings

Thermogravimetric analysis was carried out to verify the actual content of GNP for both configurations. It is worth considering that even if the base coat layer is heavily loaded with GNP the filler content measured by the TGA analysis is an average estimation across all the multilayer films.
The actual GNP content was determined through thermogravimetric analysis (TGA) at 750 °C, where the neat polymer exhibited a dry residue of 7.4 wt %. The measured residue of each nanocomposite was corrected by subtracting the residue of the neat polymer above. The effective filler content was then calculated by normalising the corrected residue to the total sample mass:

$$\%w_{f,real} = \frac{\%w_c - \%w_{NR}}{100 - \%w_{NR}} \cdot 100 \qquad \text{(Eq. 1)}$$

The multilayer content is 2.2 wt % for G2Nan and 14.8 wt % for G7Nan. The DSC and TGA results are summarized in Table 3.

Table 3. Thermal Analysis results on the standard and GNP modified finishing layers

SAMPLE	NOMINAL FILLER (wt%)	RESIDUE (wt%)	FILLER CONTENT (wt%)	FILLER CONTENT (VOL%)	Tg_0 (°C)	Tg (°C)
Neat	0.0	7.4	0.0	0.0	-31.81	78.76
G2	4.0	9.5	2.2	1.0	-31.74	77.37
G7	18.0	14.8	8.0	4.6	-28.66	73.73

The actual filler contents are in line with the expected values. In the case of G7Nan-based nanocomposite, the expected content is 8.6 wt % (1.44 g / 16.8 g, see Table 2) while the actual content is 8.0 wt % according to the method defined by (Yee and Stephens 1996). Similarly, the G2Nan-based film is 2.2 wt % compared to the expected content of 2.1 wt % (0.36 g / 16.8 g).
Differential scanning calorimetry revealed the presence of two distinct glass transition temperatures (Tg) in the multilayer polyurethane systems: a low-temperature transition ($Tg_0 \approx -32$ °C) associated with the

soft segments and a higher transition (Tg ≈ 78 °C) attributed to the hard segment domains. The incorporation of graphene nanoplatelets (GNPs) induced only minor changes in the soft segment Tg_0, suggesting limited disruption of the flexible phase microstructure. In contrast, the hard-segment Tg decreased progressively with increasing GNP content and decreasing lateral size: from 78.8 °C in the neat coating to 77.4 °C for G2Nan (4.5 wt %, larger aspect ratio) and 73.7 °C for G7Nan (18.0 wt %, smaller aspect ratio). This reduction likely originates from the interference of GNPs with the hydrogen-bonded hard-segment network, reducing phase separation and promoting a certain degree of plasticization. Higher GNPs loadings combined with smaller lateral sizes favor agglomeration and limit effective interfacial bonding, thereby lowering the degree of hard-domain connectivity. These observations align with literature indicating that while GNPs can reinforce polyurethane matrices, they may also disturb the hard-segment packing and domain continuity, depending on filler morphology and dispersion quality (Vallés *et al*., 2015; Agustina *et al*., 2023; Naji *et al*., 2025).

The tensile strength and elongation at break are crucial parameters for assessing the durability and flexibility of the material. These tests have the scope to evaluate possible variations in the mechanical properties and deformability of the nanocomposite multilayer finish compared to the neat polymer, to identify potential issues related to deformation compatibility with the leather substrate, which could render the coating unsuitable for automotive applications. The stress–strain curves at 23 °C and 60 °C (Figure 2) show an initial quasi-linear elastic region, followed by a progressive plastic deformation characterized by permanent set and gradual stress stabilization. Before failure, the films exhibit an extended deformation stage where the stress remains nearly constant or slightly increases due to strain-induced orientation of the soft segments. The final drop corresponds to film rupture, marking the maximum stress point and ultimate breakage.

At 23 °C (Figure 2.a), the GNP-filled coatings show an increase of coating stiffness and a slight increase in tensile strength using both GNPs. Since the polyurethane matrix is sensitive to temperature variations, tests were also conducted at 60 °C (in Figure 2.b). The curves display the same elastic-plastic behaviour with a slight reduction of stiffness and tensile strength. At both test temperatures, G2Nan resulted in a slight increase in elongation at break while G7Nan determines a slight decrease, more evident at higher temperatures (60 °C).

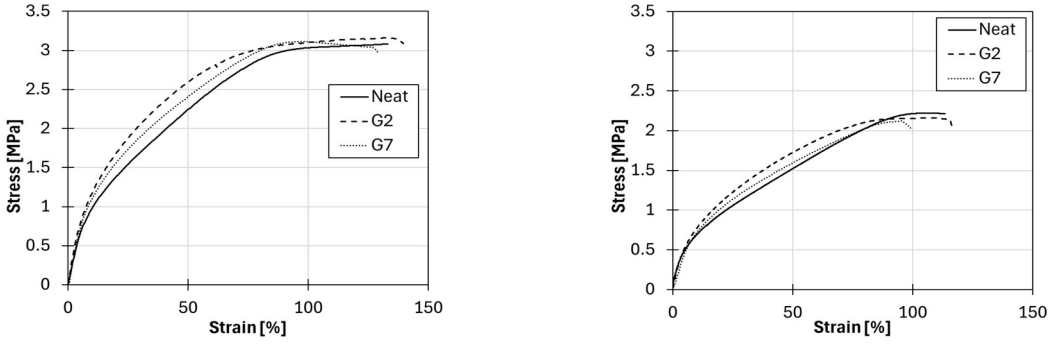

Figure 3 – Tensile test on finishing film, (a) at room temperature, (b) at 60 °C degree

3.2 Nanoindentation results on finished leathers

The sample was mapped on a grid with a Z offset of -50 µm and a Y offset of 15 µm, allowing exploration of the mechanical properties at specific points on the sample for a more detailed and representative analysis. The measurement of indentation depth and the applied force provide data on the mechanical properties. The results were analysed by comparing the mechanical properties between the two types of leather (with and without functionalized coating), evaluating hardness, elastic modulus, and wear resistance.

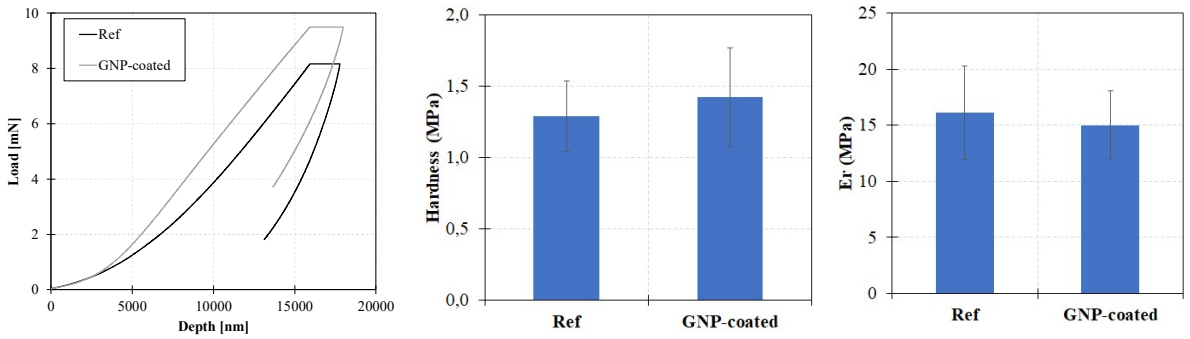

(a) *(b)* *(c)*

Figure 4 – Nanoindentation tests on standard samples and GNP modified finished layer

Figure 4.a shows the force-depth curves from the indentation tests on leather samples with and without the G2Nan functionalized coating. It can be observed that leather treated with GNP exhibits higher hardness compared to traditionally tanned leather. In particular, the bar diagrams show an increase in 10 % in hardness and the 7 % reduction in elastic modulus (Figure 4.b and 4.c). Higher hardness values indicate greater resistance to deformation, suggesting that the graphene nanoplatelets enhance the mechanical resistance and durability of the coatings, confirming the results of tensile tests.

3.3 Thermal conductivity performance of leather finished with nanocomposite multilayer

In Figure 5 a detail of leather surfaces coated using finishings loaded with G7Nan (a) and G2Nan (b) multilayer nanocomposites is shown.

(a) *(b)*

Figure 5 - Surface of G7Nan (a) and G2Nan (b) nanocomposite base coats

The correlation between the spatial temperature distribution on a surface and the thermal diffusivity of the material is key to understanding the material's heat transfer capacity. Thermal diffusivity describes the rate at which heat spreads through a material. Although the LED test is not quantitative, it allows for a qualitative evaluation of the effects of the functionalized coating on heat dissipation.
When a heat source, such as an LED, is applied to a surface, the speed and the mode of heat transfer depend spatially on the thermal diffusivity. Materials with high thermal diffusivity show a more rapid and uniform temperature distribution, while materials with low diffusivity tend to develop sharper temperature gradients near the heat source. The thermal diffusion equation for the temperature T(x, t) along a distance x and as a function of time t is defined by:

$$\frac{\partial T}{\partial t} = \alpha \frac{\partial^2 T}{\partial x^2} \qquad \text{(Eq. 2)}$$

This model can be used to analyse the thermal behaviour by measuring the temperature distribution at successive times, allowing an estimation of the material's thermal diffusivity.

Figure 6 displays IR images from the LED test conducted on leather samples without GNP coatings (neat coating). In Figure 6.a (test 1), the temperature value at the edge of the surface in contact with the heat source is reported, while in Figure 6.b, the temperature on the opposite side after applying the heat source (cross-plane, test 2) is shown.

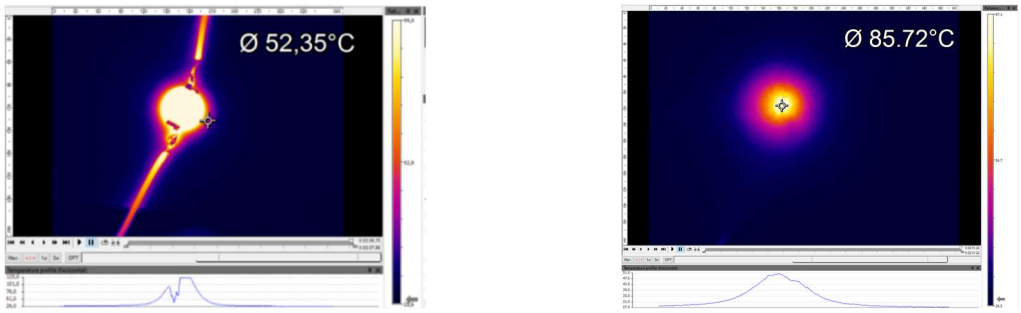

(a) *(b)*

Figure 6 – Temperature distribution on neat leather finishing in-plane test (a) and cross-plane test (b)

Furthermore, Figure 7 shows test results on G2Nan nanocomposite finishing. It can be observed that in both the tests (in-plane and cross-plane set-up), the temperatures over the GNP-coated specimen are lower compared to the neat sample.

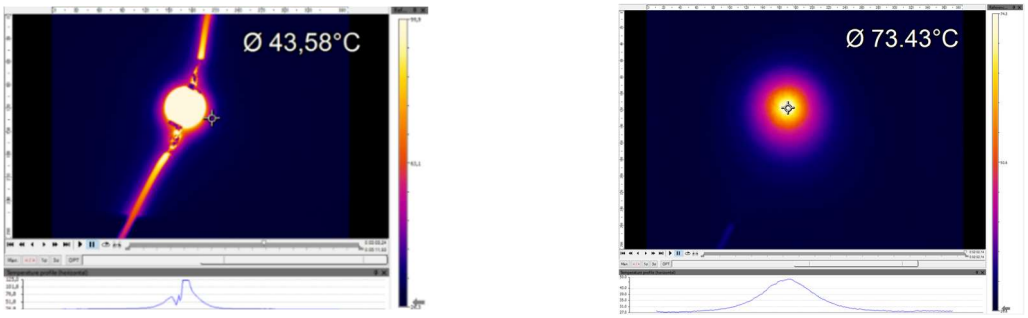

(a) *(b)*

Figure 7 – Temperature distribution on leather finishing with GNP modified finishing layer

For the cross-plane configuration, Figure 8 illustrates the temperature evolution over time at two positions: at the centre of the heat source and at point located 30 pixels away.

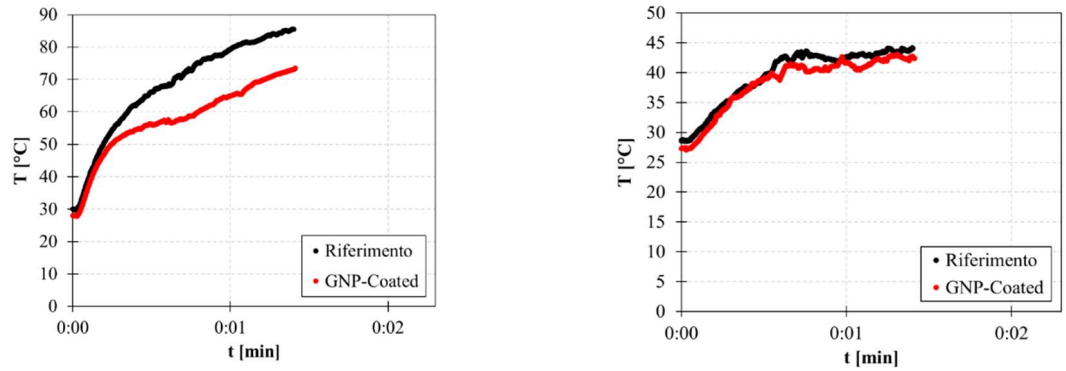

(a) *(b)*

Figure 8. Temperature vs time in Test 2: (a) central point and (b) 30 pixels far from the source

The images show that, at the centre of the heating source (Figure 8.a), the temperature of both samples (neat and G2Nan-loaded) initially increases at a rate of approximately 20 °C/min. Subsequently, the two profiles diverge, with the G2Nan-loaded coating reaching a temperature approximately 15 °C lower than the neat sample after 5 seconds. At a position 30 pixels away from the centre (Figure 8.b), G2Nan coatings exhibits again a slightly lower temperature than the neat sample. These results suggest that the thermal diffusivity of the material is influenced by its microstructure, particularly by the incorporation of conductive GNP nanofillers. Materials with higher thermal diffusivity spread heat more rapidly, whereas those with lower diffusivity offer greater resistance to heat propagation.

4 Conclusions

In this study, two types of graphene nanoplatelets (GNPs) with different aspect ratios (approximately 1500 and 500) were incorporated into the finishing layer of automotive leather to create a multilayer functional coating designed to enhance the mechanical performance of the finishing layer and, simultaneously, improve surface thermal conductivity and thereby improving thermal comfort. The proposed finishing system consists of a multilayer coating in which only the base coat was modified with GNPs. The GNP content was selected to exceed the percolation threshold, ensuring a significant improvement in both thermal and electrical conductivity. In both cases, the aesthetic requirements were preserved by applying a conventional topcoat, while the functional base layer contributed to enhanced overall performance. The GNP-modified coatings exhibited increased surface hardness, while the elastic modulus showed a slight decrease, likely due to local nanoparticle agglomeration. A dedicated experimental setup was developed for non-destructive evaluation of thermal diffusion. A controlled-power LED source was applied in contact with both the top and back layers of the finished leather, revealing a clear increase in thermal diffusivity for the GNP-modified finishing layer compared to the neat system.

5 Acknowledgements

Activities have been carried out in the framework of LEONARDO – Solutions for driving comfort and vehicle performance efficiency, project ID B32C18000340007. LEONARDO is part of BORGO4.0, a project financed by the Campania Region POR FESR 2014/2020 action lines. The authors would like to thank to Fabio Docimo for his support in experimental characterization.

6 References

- Agustina, E., Goak, J. C., Lee, S., Kim, Y., Hong, S. C., Seo, Y. & Lee, N. (2023).
- Effect of Graphite Nanoplatelet Size and Dispersion on the Thermal and Mechanical Properties of Epoxy Based Nanocomposites. Nanomaterials, 13(8), art. 1328. https://doi.org/10.3390/nano1308132
- Cilento, Fabrizia, Alfonso Martone, Maria Giovanna Pastore Carbone, Costas Galiotis, and Michele Giordano. 2021. 'Nacre-like GNP/Epoxy Composites: Reinforcement Efficiency Vis-à-Vis Graphene Content'. Composites Science and Technology 211:108873. doi:10.1016/J.COMPSCITECH.2021.108873.
- Fan, Qianqian, Jianzhong Ma, and Qunna Xu. 2019. 'Insights into Functional Polymer-Based Organic-Inorganic Nanocomposites as Leather Finishes'. Journal of Leather Science and Engineering 1(1):1–10. doi:10.1186/S42825-019-0005-9/FIGURES/8.
- Jakhmola, Swati, Sonalee Das, and Kingshuk Dutta. 2024. 'Emerging Research Trends in the Field of Polyurethane and Its Nanocomposites: Chemistry, Synthesis, Characterization, Application in Coatings and Future Perspectives'. Journal of Coatings Technology and Research 21(1):137–72. doi:10.1007/S11998-023-00841-Z/METRICS.

- Kaur, Ravinder, Sanjeev Kumar Verma, and Rajeev Mehta. 2025. 'Tailoring the Properties of Polyurethane Composites: A Comprehensive Review'. Polymer-Plastics Technology and Materials. doi:10.1080/25740881.2025.2493869;
- Kiranakumar. H. V, Thejas R, Naveen C S, M. Ijaz Khan, Prasanna G D, Sathish Reddy, Mowffaq Oreijah, Kamel Guedri, Omar T. Bafakeeh, and Mohammed Jameel. 2024. 'A Review on Electrical and Gas-Sensing Properties of Reduced Graphene Oxide-Metal Oxide Nanocomposites'. Biomass Conversion and Biorefinery 14(12):12625–35. doi:10.1007/S13399-022-03258-7/METRICS.
- Kothandam, Ramkumar, Muthuraman Pandurangan, R. Jayavel, and Sanjeev Gupta. 2016. 'A Novel Nano-Finish Formulations for Enhancing Performance Properties in Leather Finishing Applications'. Journal of Cluster Science 27(4):1263–72. doi:10.1007/S10876-016-0997-8/TABLES/6.
- Mohamed, O. A., A. B. Moustafa, M. A. Mehawed, and N. H. El-Sayed. 2009. 'Styrene and Butyl Methacrylate Copolymers and Their Application in Leather Finishing'. Journal of Applied Polymer Science 111(3):1488–95. doi:10.1002/APP.29022.
- Naji, H. Z., Albozahid, M., Alobad, Z. K., & Saiani, A. (2025, 30 giugno). Size effects of the graphene nanoplatelets on the thermal and tensile properties of segmented thermoplastic polyurethane nanocomposites. Composite Interfaces, online ahead of print. https://doi.org/10.1080/09276440.2025.2525594
- Pharr, G. M., & Oliver, W. C. (July 1992). "Measurement of Thin Film Mechanical Properties Using Nanoindentation." MRS Bulletin, Vol. 17, No. 7, pp. 28–33.
- DOI: 10.1557/S0883769400041634
- Sharma, Rahul, Harish Kumar, Diksha Yadav, Chetna Saini, Rajni Kumari, Gaman Kumar, Aravind Babu Kajjam, Vaidehi Pandit, Mehnaz Ayoub, Saloni, Yogesh Deswal, and Ashok K. Sharma. 2024. 'Synergistic Advancements in Nanocomposite Design: Harnessing the Potential of Mixed Metal Oxide/Reduced Graphene Oxide Nanocomposites for Multifunctional Applications'. Journal of Energy Storage 93:112317. doi:10.1016/J.EST.2024.112317.
- Soon, Li Jie, Tuti Katrina Abdullah, Amira Sofea Mahamad Husin, and Syazana Ahmad Zubir. 2025. 'Enhanced Hydrophobicity of Polyurethane Coating for Steel Protection through Replication and Nanomaterial Integration'. Journal of Thermoplastic Composite Materials 38(6):2120–37. doi:10.1177/08927057241292303.
- Vallés C., Beckert F., Burk L., Kinloch I. A., Young R. J.
- "The effect of flake diameter on the reinforcement of few layer graphene–PMMA composites." Composites Science and Technology, vol. 111, pp. 17–22 (2015).
- DOI: 10.1016/j.compscitech.2015.02.022
- Yee, R. Y., and T. S. Stephens. 1996. "A TGA Technique for Determining Graphite Fiber Content in Epoxy Composites". Thermochimica Acta 272(1–2):191–99. doi:10.1016/0040-6031(95)02606-1.
- Zheng, Jie, Philip R. Nicovich, and Robert M. Dickson. 2007. 'Highly Fluorescent Noble-Metal Quantum Dots'. Annual Review of Physical Chemistry 58(Volume 58, 2007):409–31. doi:10.1146/.58.032806.104546.